



CPPM seminar

12.11.2025

Simulation of hybrid pixel detectors: Validation with XPAD3.2-S/CdTe measurements

Mélissa Leroy^{1,2}, Mathieu Dupont¹, Elena Gaborieau-Borissenko², Yannick Boursier¹, Christian Morel¹

¹ Aix Marseille Univ, CNRS/IN2P3, CPPM, Marseille, France

² Detection Technology, 38430 Moirans, France

melissa.leroy@deete.com

mleroy@cppm.in2p3.fr

1. Context of the thesis

- **Detection Technology company:**



Medical X-ray imaging

Computed tomography
Dental imaging
Surgical imaging



Security X-ray imaging

Baggage and parcel scan
Cargo and vehicle scan
People scan



Industrial X-ray imaging

Food industry
Recycling and sorting
Mining industry

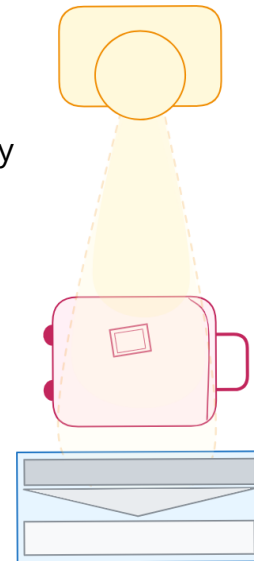
- One axis of the strategy: develop **Spectral Photon Counting solutions**
- Build an **X-ray chain simulator** as an internal research and development tool for the company

- **Thesis:**

- **Detection Technology (DT)** leverage the simulation expertise of **imXgam team (CPPM)**
- Focus on the **simulation of X-ray Photon Counting Spectral Detectors**


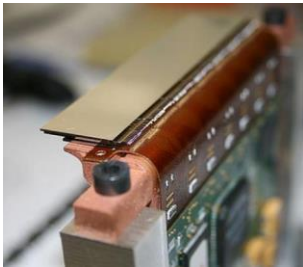

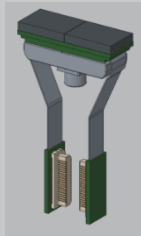
- **Motivation for a simulation of hybrid pixel detectors**

- Early stage of development: detector design optimization
- Detector operation optimization
- Create a database for Machine Learning methods
- Development of correction algorithms
- **Fundamental physics insight of the detector behavior and limitation factors**



1. Context of the thesis

• Detectors used for the study

Detectors	<u>Amptek: XR-100T-CdTe</u>	<u>CPPM: XPAD3.2-S/CdTe</u>	<u>DT: X-Card ME3</u>	<u>DT: Prototype</u>
				
Characteristics	<ul style="list-style-type: none"> • Mono-pixel detector • 3 mm pitch • Cadmium Telluride • 1 mm thickness 	<ul style="list-style-type: none"> • 2D Matrix • 130 μm pitch • Cadmium Telluride • 750 μm thickness 	<ul style="list-style-type: none"> • Linear detector of 128 pixels • 800 μm pitch • Cadmium Telluride • 2 mm thickness • Up to 128 bins 	<ul style="list-style-type: none"> • 2D Matrix • 2x 24x36 pixels • 350 – 400 μm pitch • Cadmium Zinc Telluride • 2 mm thickness • Up to 6 bins
Impact on simulation development	Reference for understanding physical processes occurring in CdTe	Validation of the simulation on experimental measurements	Generalization of the simulation's model to another detector	Test simulation prediction abilities to anticipate measurement campaign

2. Simulation framework

a. X-ray interactions

X-ray
interactions

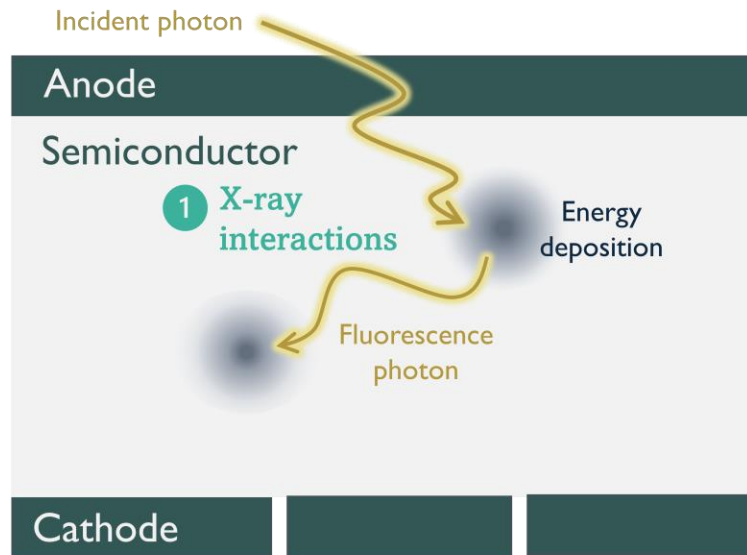
Carrier generation

Charge carrier
dynamics

Charge carrier
collection

Material	Total	Photoelectric	Compton	Rayleigh
Si (50 mm)	0.94	0.28	0.56	0.1
CdZnTe (1.6 mm)	0.94	0.87	0.04	0.04
CdTe (1.6 mm)	0.94	0.89	0.03	0.02

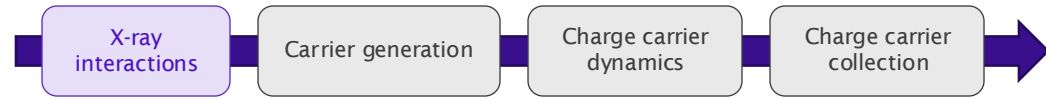
Material		Z	$K_{\alpha 1}$ [keV]	$K_{\alpha 2}$ [keV]	$d_{\alpha 1}$ [μm]	$d_{\alpha 2}$ [μm]
Si		14	1.74	1.74	11.86	11.86
Ge		32	9.89	9.86	50.85	50.40
GaAs	Ga, 48.20%	31	9.25	9.22	40.62	40.28
	As, 51.80%	33	10.54	10.50	15.62	15.47
CdTe	Cd, 46.84%	48	23.17	22.98	113.20	110.75
	Te, 53.16%	52	27.47	27.20	59.32	57.85



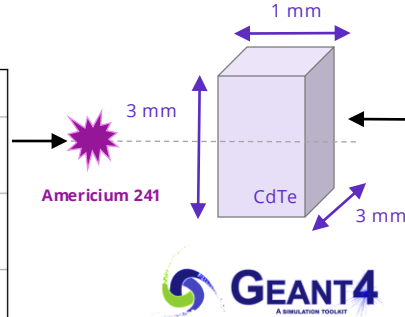
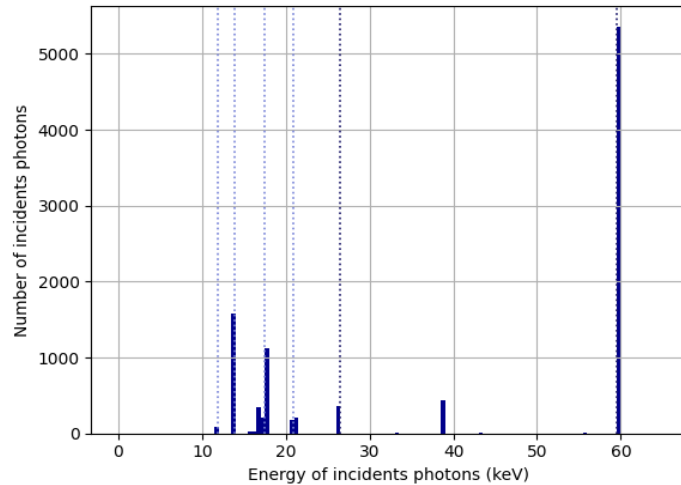
2. Simulation framework

a. X-ray interactions

- Tracking of particles in the sensor, their position and energy loss
- Photoelectric effect, Compton scattering
- CdTe : fluorescence escape photon



Americium 241 source



Amptek : XR-100T-CdTe

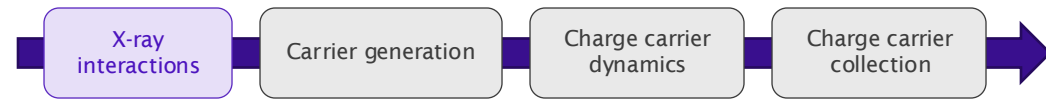


- Mono-pixel detector
- CdTe
- 3 mm pitch
- 1 mm thickness

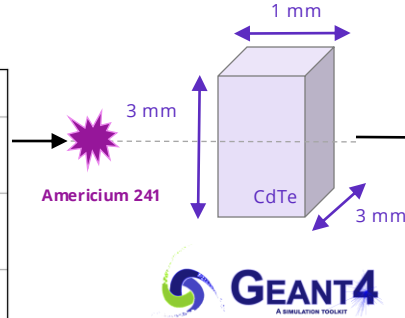
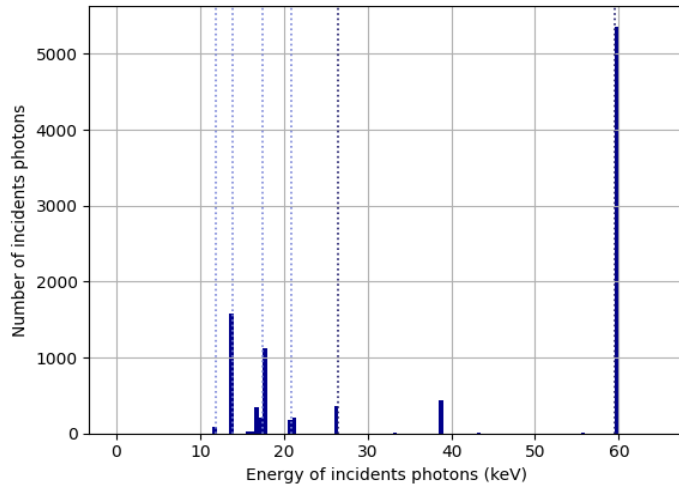
2. Simulation framework

a. X-ray interactions

- Tracking of particles in the sensor, their position and energy loss
- Photoelectric effect, Compton scattering
- CdTe : fluorescence escape photon



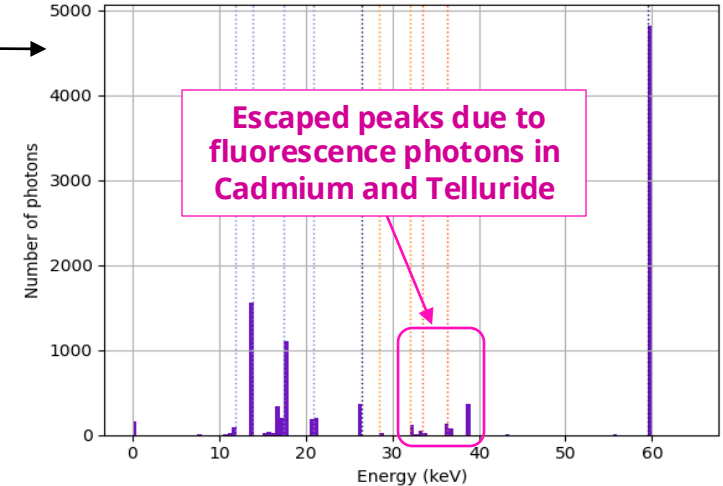
Americium 241 source



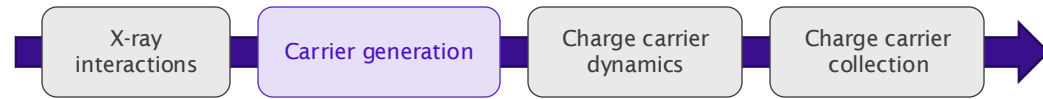
Spectral response in a bulk of Cadmium Telluride

x = 3.0 mm, y = 3.0 mm and z = 1.0 mm

source : Am 241



2. Simulation framework



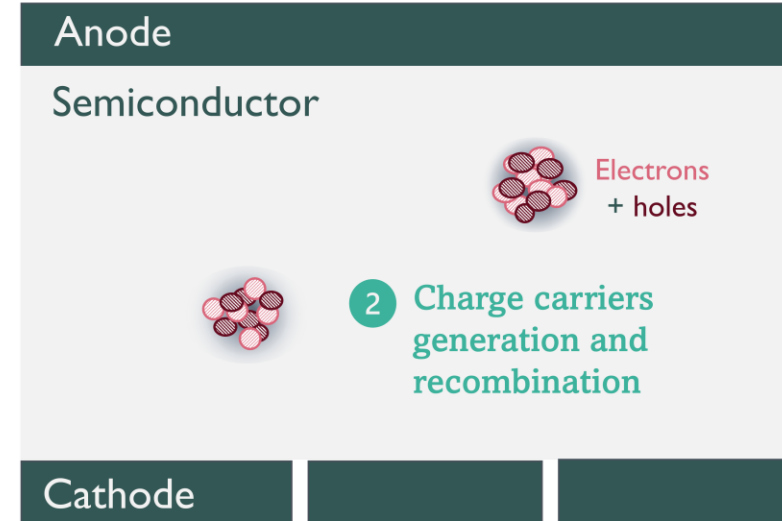
b. Carrier generation and recombination

- Number of e-h generated depends on the material of the sensor
- This number fluctuates (gaussian distribution)

$$\mu = N$$
$$\sigma = \sqrt{FN}$$

N: Number of charges created
F: Fano factor

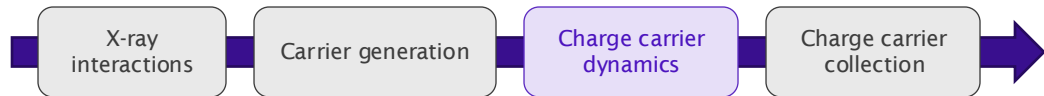
Material		$E_{e/h}$	Fano factor
Cadmium Telluride	CdTe	4.43 eV	0.24
Cadmium-Zinc Telluride	CdZnTe	4.64 eV	0.14
Silicon	Si	3.64 eV	0.115



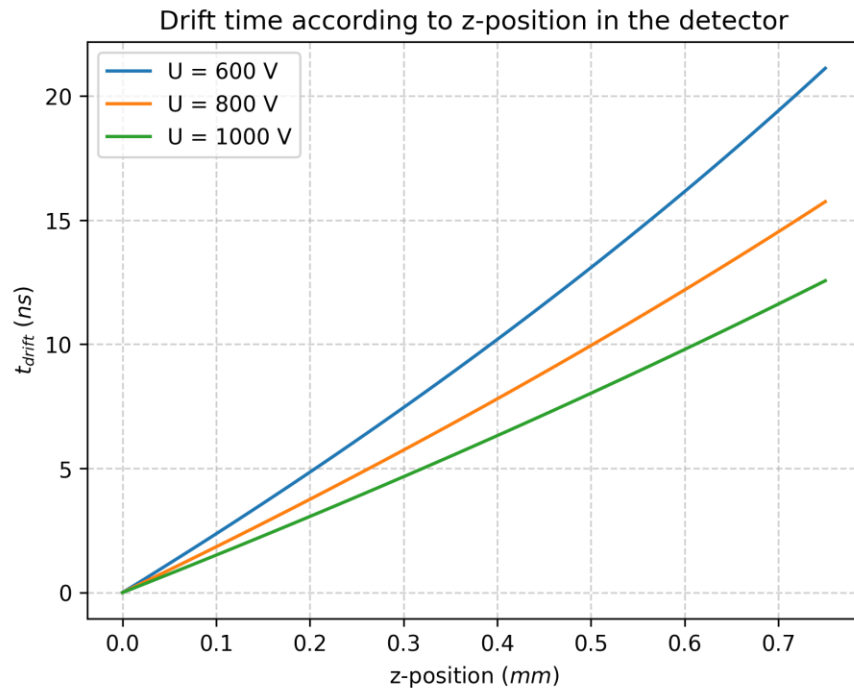
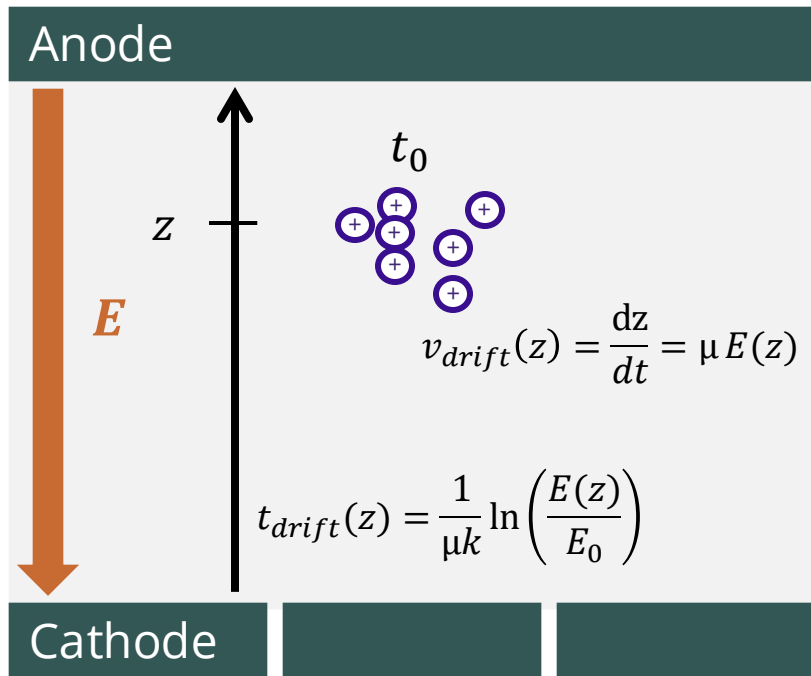
- It is the intrinsic limitation in energy resolution of the detector

2. Simulation framework

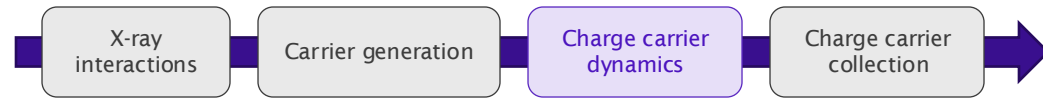
c. Charge carrier dynamics



- Charges drift toward the electrodes under the influence of electric field



2. Simulation framework



c. Charge carrier dynamics

- Diffusion and repulsion cause a spontaneous spread of charge carriers
- If size of the electronic cloud increase it may induce **charge sharing**

Charge continuity equation

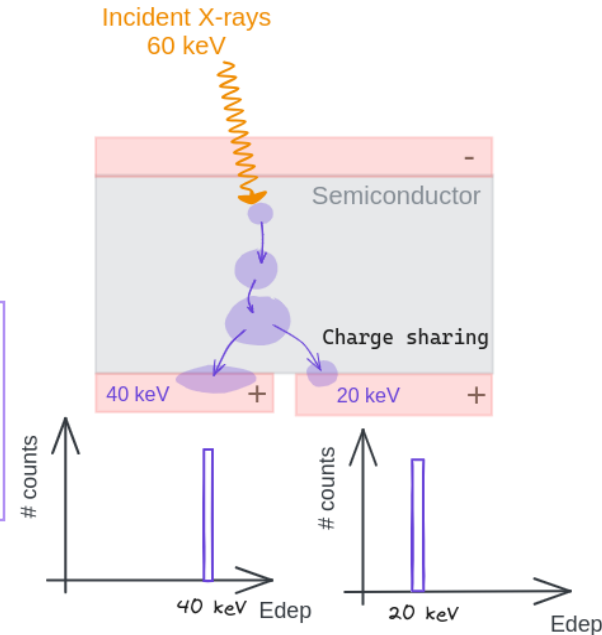
- Concentration of charge carrier evolution with respect to space and time
- Neglecting generation and recombination at $t > 0$:

$$\frac{\partial \rho}{\partial t} = \underbrace{D \nabla^2 \rho}_{\text{Diffusion}} - \underbrace{\mu \nabla \cdot (\rho \mathbf{E})}_{\text{Electrostatic repulsion}}$$

ρ : Density of charges
 D : Diffusion coefficient
 μ : Mobility of charge carriers
 \mathbf{E} : Electric field induced by charge carriers

Equation solving

- Complex + time consuming in simulation: approximation of the solution using models



2. Simulation framework

c. Charge carrier dynamics

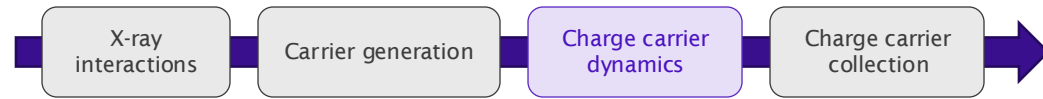
- The 2 models studied :

- Repulsion and diffusion are **independents**

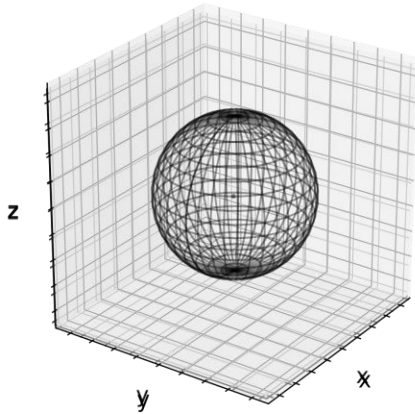
E. Gatti et al., NIMA, 253 (1987) 393-399, DOI: 10.1016/0168-9002(87)90522-5.

- Repulsion and diffusion are **dependents**

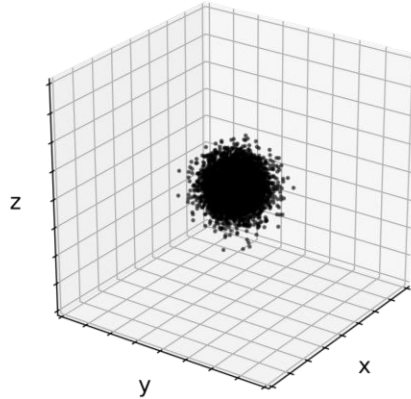
M.Benoit et al., NIMA, 606 (2009) 508-516, DOI: 10.1016/j.nima.2009.04.019.



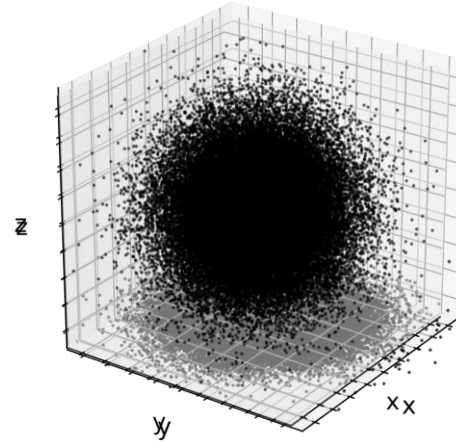
Spheric electronic cloud
 $t = t_0$



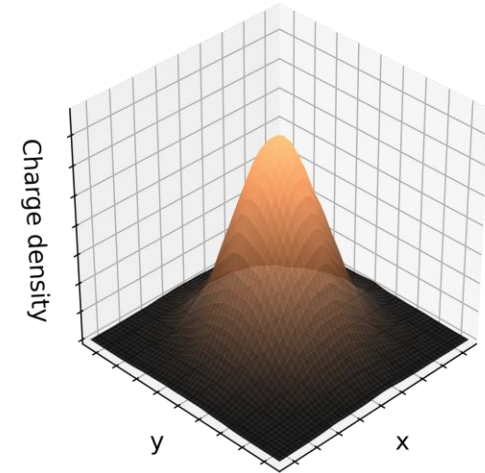
$t = t_1$



Projection on XY electrodes plan
 $t = t_{drift}$



Charge density



2. Simulation framework

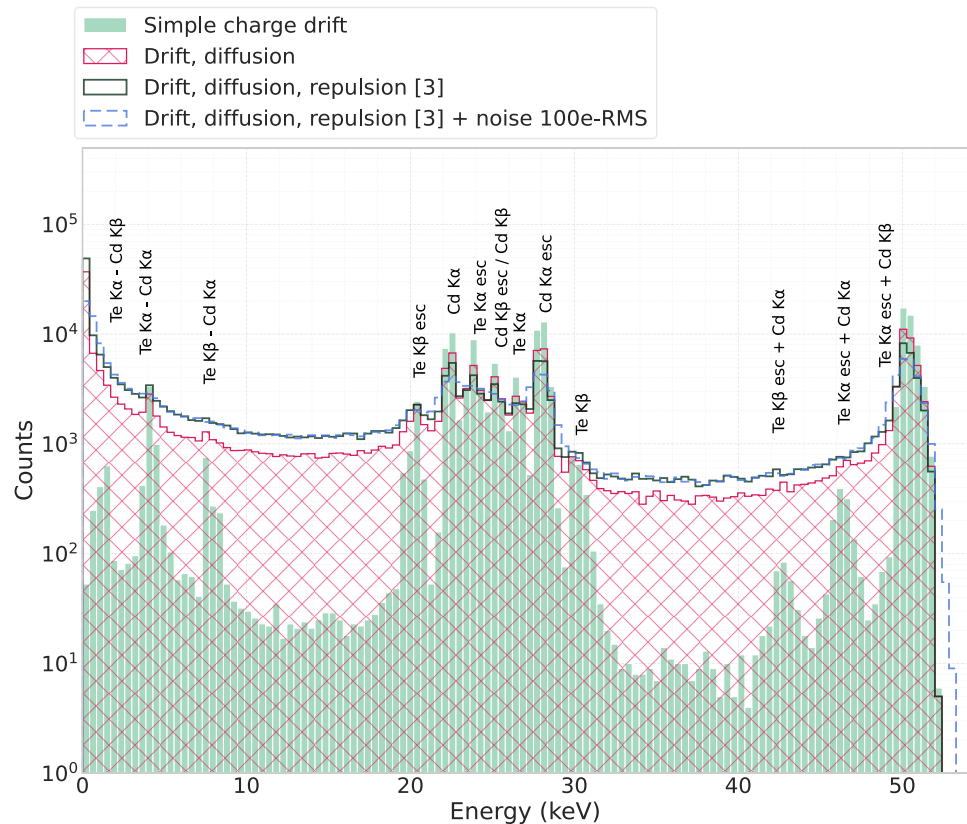
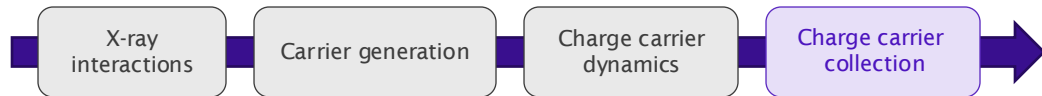
c. Charge carrier collection

- Electronic noise approximated by a convolution with a gaussian

Simulation parameters

Holes mobility	100 cm ² /(V.s)
holes lifetime	2 μs
Fano factor	0.24
Incident beam energy	52 keV

- Fluorescence escape peaks are visible on the spectrum
- The full energy peak is shifted due to an incomplete collection of charges
- Activation of diffusion and repulsion increase the size of the electronic cloud and so the charge sharing

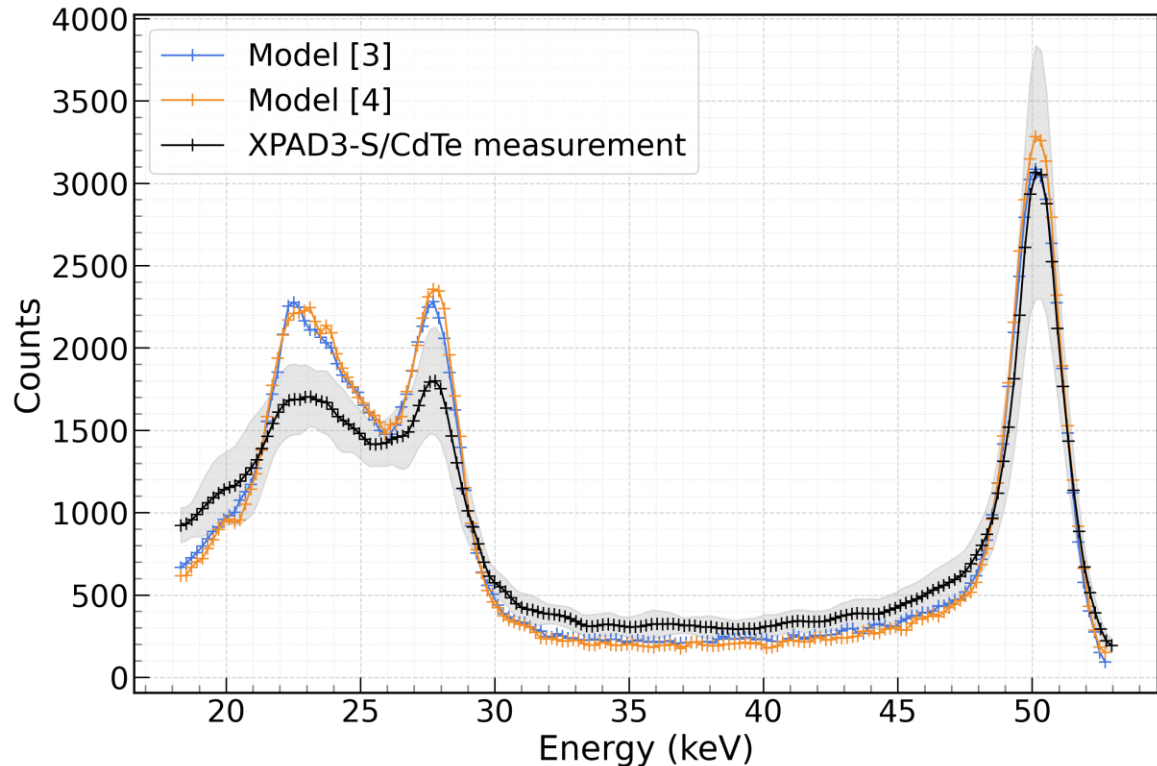


3. Experimental validation

c. Comparison of simulation and experimental measurements

- Model [3]: **independent**
- Model [4]: **dependent**

- Reasonable agreement is observed between the simulations and the mean experimental spectrum
- A higher electronic noise was set to match experimental measurements (close to 170 e⁻ RMS)
- Discrepancies sources can be caused by a non uniform distribution of the threshold steps and some phenomenon are not simulated (pile-up)



4. Conclusion

a. Summary



Goals of the study:

- Development of a simulator capable to reproduce the radiographic chain
- Focus on the simulation of photon counting pixel detector
- Reproduction of the causes of spectral distortion:
 - Fluorescence escape
 - Charge sharing

Method:

- Development of a simulator integrating charge carrier generation, trapping, dynamics
- Study of 2 charge transport models, essential to reproduce charge sharing
- Processing of XPAD3.2-S/CdTe measurement performed in synchrotron
- Reasonable agreement found between simulation and experimental measurements

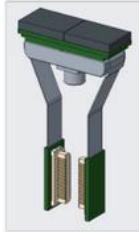
Prospects:

- Application of the simulator to other detectors to test its robustness and refine the comparison with experimental data
- Integration of charge induction currently absent from the simulator, to improve the accuracy of the results

4. Conclusion

b. Next steps

DT : Prototype



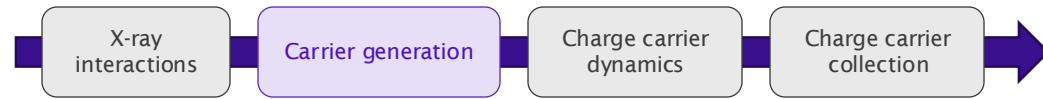
- 2D Matrix
- 2x 24x36 pixels
- 350 – 400 μm pitch
- Cadmium Zinc Telluride
- 2 mm thickness
- Up to 8 bins



- Simulator to be validated against experimental data of CdTe and CZT hybrid pixels prototypes developed by Detection Technology
- ESRF measurement campaign planned from the 10th to 14th December 2025

Thank you

2. Simulation framework



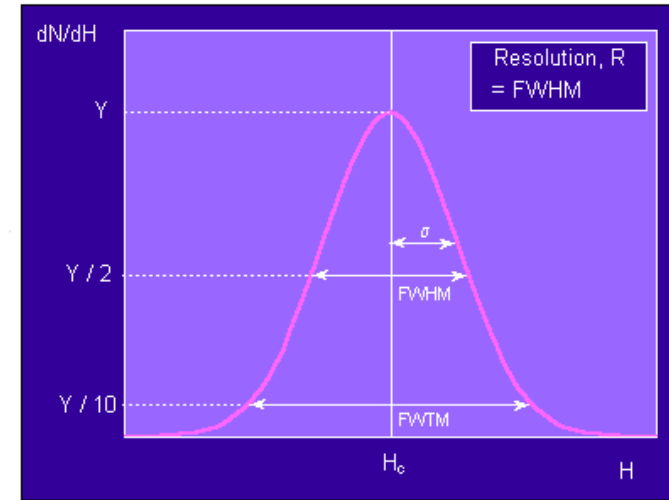
b. Carrier generation and recombination

- In theory, the variance in the number of charge carriers should follow a stochastic behaviour and therefore a Poisson statistics
- But in reality this is a deterministic problem and in real detectors, the observed variance is usually smaller than the one predicted by Poisson statistic.
- Fano factor is the ratio between observed variance and Poisson predicted variance.

$$F = \frac{\text{Observed variance } N}{\text{Poisson variance } (N)}$$

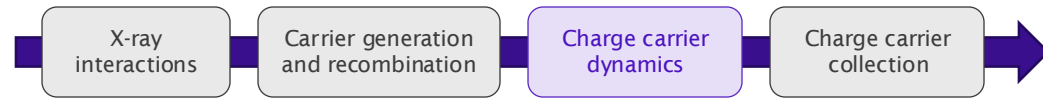
- Resolution limit: the statistical limit of energy resolution is:

$$R = 2.35 \sqrt{\left(\frac{F}{N}\right)}$$



2. Simulation framework

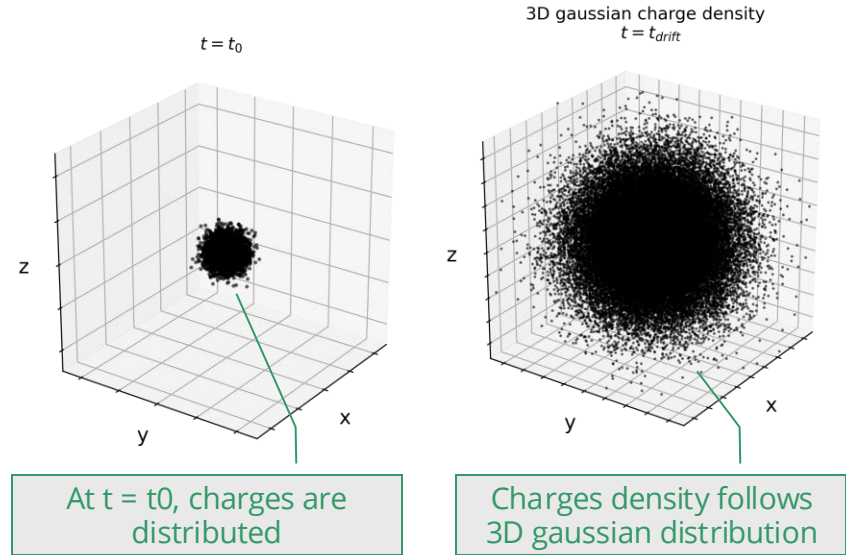
c. Charge carriers dynamics



Model 2: Coupling repulsion and diffusion

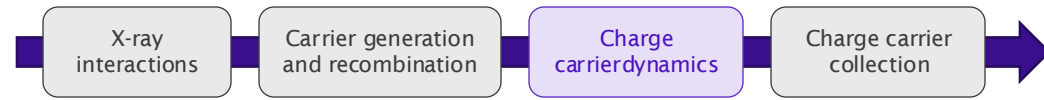
$$\frac{\partial \rho}{\partial t} = \underbrace{D \nabla^2 \rho}_{\text{Diffusion}} - \underbrace{\mu \nabla \cdot (\rho \mathbf{E})}_{\text{Electrostatic repulsion}}$$

$$\frac{d\sigma^2(t)}{dt} = 2 \underbrace{\left(D + \frac{\mu N q_e}{24 \pi^{3/2} \epsilon_0 \epsilon_r \sigma(t)} \right)}_{D_{eff}} = 2 D_{eff}$$



2. Simulation framework

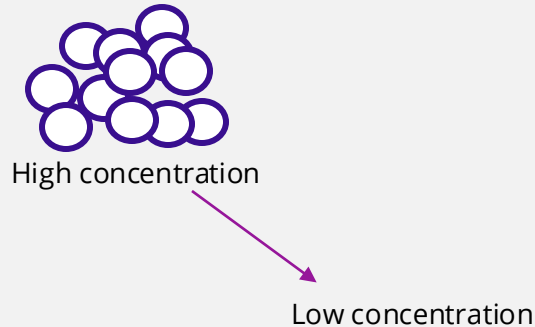
c. Charge carrier dynamics



- Diffusion and repulsion cause a spontaneous spread of charge carriers

Diffusion

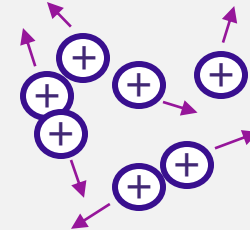
○ Electrons/Holes



An inhomogeneous distribution induces a spontaneous Brownian motion

Repulsion

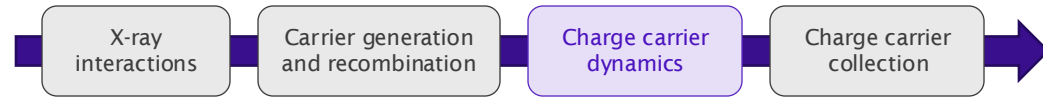
⊕ Holes



Charges of the same sign repel each other due to electrostatic forces

2. Simulation framework

c. Charge carriers dynamics



Model 1: Decoupling repulsion and diffusion

$$\frac{\partial \rho}{\partial t} = \underbrace{D \nabla^2 \rho}_{\text{Diffusion}} - \underbrace{\mu \nabla \cdot (\rho \mathbf{E})}_{\text{Electrostatic repulsion}}$$

Diffusion-only equation:

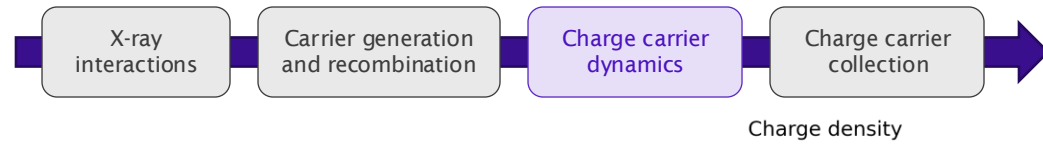
$$\frac{\partial \rho}{\partial t} = D \nabla^2 \rho$$

Repulsion-only equation:

$$\frac{\partial \rho}{\partial t} = -\mu \nabla \cdot (\rho \mathbf{E})$$

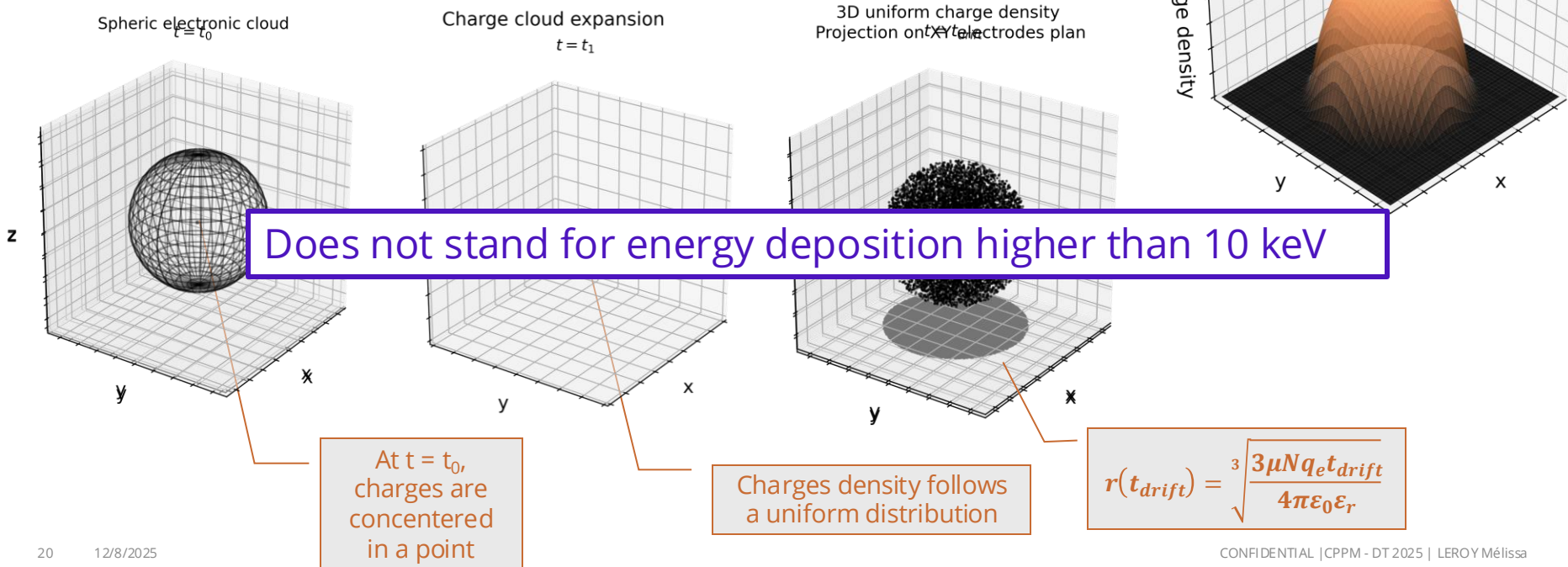
2. Simulation framework

c. Charge carriers dynamics



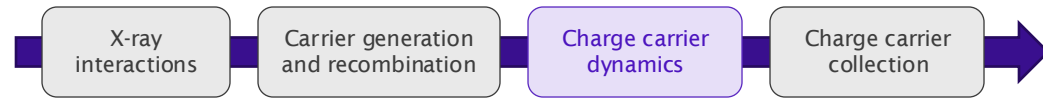
Model 1: Decoupling repulsion and diffusion

- Repulsion-only equation: $\frac{\partial \rho}{\partial t} = -\mu \nabla \cdot (\rho \mathbf{E})$
- For a **spherical** symmetry, the **repulsion** cause the electronic cloud to extend and $r(t) \propto \sqrt[3]{t}$



2. Simulation framework

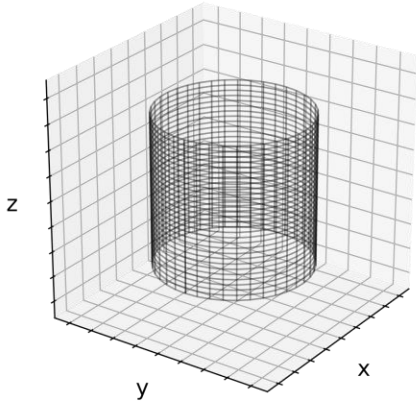
c. Charge carriers dynamics



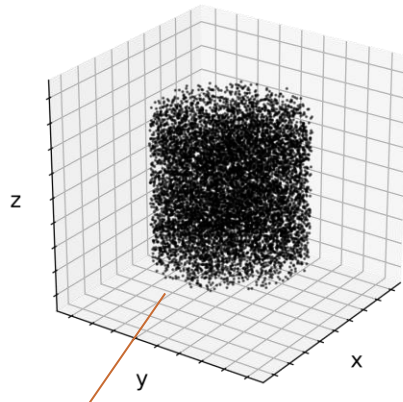
Model 1: Decoupling repulsion and diffusion

- For a **cylindric** symmetry, the **repulsion** cause the electronic cloud to extend and $r(t) \propto \sqrt[2]{t}$

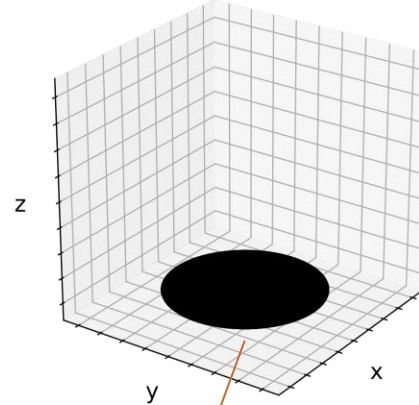
cylindric electronic cloud



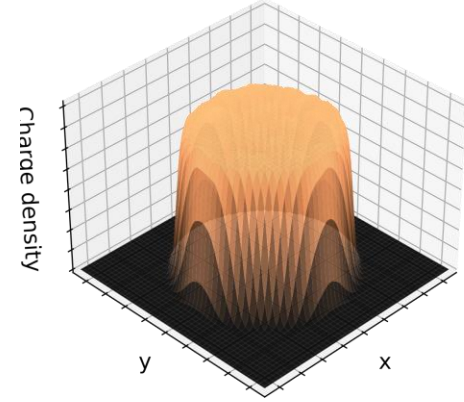
3D uniform density



Projection on XY electrodes plan



Charge density



Charges density follows
a uniform distribution

$$r(t_{\text{drift}}) = \sqrt{q_e \frac{S_{\text{LOSS}} \mu_0 t_{\text{drift}}}{E_{\text{eh}} \pi \epsilon}}$$

3. Experimental validation

b. Experimental measurements processing

- Calibration for each pixels
- Average over 536 pixels

